# Chronopotentiometric Measurement of Adsorption. Riboflavin on a Mercury Electrode

SHANKAR V. TATWAWADI and ALLEN J. BARD

*Department of Chemistry, The University of Texas, Austin, Texas*

▶ From the variation of $i_o\tau^{1/2}/C$ with $\tau$ during the chronopotentiometric reduction of riboflavin, the amount of riboflavin adsorbed on the electrode, $\Gamma$, is calculated. Values of $\Gamma$ calculated using various theoretical models are discussed, and these values are compared to the one deduced from electrocapillarity measurements.

ADSORPTION of the electroactive species causes the value of the chronopotentiometric constant, $i_o\tau^{1/2}/C$, to increase with decreasing transition times. This increase in $i_o\tau^{1/2}/C$ is caused by the distribution of the current between electrolysis of the electroactive species diffusing to the electrode, for which $\tau^{1/2}$ varies as $1/i_o$, and electrolysis of the electroactive species adsorbed on the electrode, for which $\tau$ varies as $1/i_o$. The relative contribution from the adsorbed species therefore increases as $\tau$ approaches zero. Several authors have considered the chronopotentiometric measurement of adsorption (*1, 2, 12, 14, 18*) but few measurements have been made by this technique. The adsorption of iodine was measured by Lorenz and Mühlberg (*15*) using heavily platinized electrodes, and by Landsberg and coworkers (*13*) using graphite electrodes. Munson (*16*) measured the adsorption of CO on platinum. In all cases, because solid electrodes are employed, the actual surface areas of the electrodes were uncertain, and the results deduced from chronopotentiometric measurements were not checked by alternate methods of measurement. This study deals with the determination of the extent of adsorption of riboflavin on a mercury pool electrode. The various models proposed to describe the chronopotentiometric electrolysis of both a diffusing and an adsorbed species were used to calculate the amount of riboflavin adsorbed, and these results were compared to those obtained from measurements on electrocapillary curves.

## EXPERIMENTAL

Chronopotentiometric measurements generally followed the previous practice (*3*). Constant current was obtained using a regulated 250-volt power supply and appropriate resistors. The mercury pool electrode was formed in a Teflon cylinder, and was always adjusted to the same height to maintain a constant projected electrode area of 3.08 sq. cm. The auxiliary electrode was platinum foil, isolated in a compartment provided with a sintered-glass disk. A saturated calomel electrode (S.C.E.) was the reference electrode. Transition times were measured from the application of the current to the cell to a preset potential automatically, using an instrument consisting of a Hewlett-Packard 522B electronic counter for time interval measurements and a trigger circuit (*9*). Measurements were made at room temperature, 24° ± 1° C.

Electrocapillary curves were determined using a dropping mercury electrode (D.M.E.) by the drop time technique of Corbusier and Gierst (*7*). A conventional polarographic capillary (Sargent) was fused onto the vertical stand tube, and the whole assembly was held immobile during a series of measurements, with the cell being removed and replaced. Care was also taken to keep the assembly free of vibration; small variations in the angle of the D.M.E. capillary and vibrations can cause erratic drop times and unreliable surface tension measurements. Drop times of 8 to 10 seconds were used.

## RESULTS

**Reduction of Cadmium(II).** To test the apparatus and determine the experimental variation of transition time data, especially at short transition times, the reduction of cadmium (II) was carried out. The data in Table I indicate no trend in $i_o\tau^{1/2}/C$ for

transition times of 0.02 to 40 seconds; a least squares analysis of a plot of $i_o\tau^{1/2}/C$ vs. $\tau^{-1/2}$ shows a slope of $0.000 \pm 0.002$ ma.-sec. per sq. cm.-m$M$.

**Reduction of Riboflavin.** The polarographic reduction of riboflavin has been studied at several different pH's (*6, 11*). A chronopotentiometric reduction wave of riboflavin at a mercury pool electrode in a sulfate-bisulfate buffer pH 2 is shown in Figure 1. Current and transition time data for the reduction of riboflavin at several different concentrations, given in Table II, show that in all cases $i_o\tau^{1/2}/C$ increases with decreasing $\tau$ (increasing $i$). Since oxide films are absent at mercury electrodes, and the variation is too large to ascribe to double layer capacity effects, the increase in $i_o\tau^{1/2}/C$ is most probably due to the reduction of riboflavin adsorbed on the electrode in addition to that diffusing from the

## Table I. Chronopotentiometric Data for Reduction of Cadmium(II)

Solution was 0.2$M$ NaClO$_4$ and 3.21m$M$ cadmium(II). Mercury pool electrode area was 3.08 sq. cm.

| $i_o$, ma. per sq. cm. | $\tau$, sec. | $i_o\tau^{1/2}/C$, ma.-sec.$^{1/2}$ sq. cm.-m$M$ |
|---|---|---|
| 0.218 | 44.6 | 0.454 |
| 0.385 | 13.7 | 0.444 |
| 1.00 | 1.81 | 0.419 |
| 3.04 | 0.22 | 0.444 |
| 6.74 | 0.043 | 0.436 |
| 10.12 | 0.0196 | 0.441 |

## Table II. Chronopotentiometric Data for Reduction of Riboflavin

Solution was 0.5$M$ NaHSO$_4$ and 1$M$ Na$_2$SO$_4$. Mercury pool electrode area was 3.08 sq. cm.

| $C$, m$M$ | $i_o$, ma. per sq. cm. | $\tau$, sec. | $i_o\tau^{1/2}/C$, ma.-sec.$^{1/2}$ sq. cm.-m$M$ |
|---|---|---|---|
| 0.800 | 0.0958 | 14.91 | 0.462 |
| | 0.1400 | 6.51 | 0.447 |
| | 0.1945 | 3.75 | 0.471 |
| | 0.2641 | 2.07 | 0.475 |
| | 0.3840 | 1.10 | 0.503 |
| | 0.5380 | 0.686 | 0.557 |
| | 1.051 | 0.299 | 0.718 |
| 0.400 | 0.0471 | 17.78 | 0.497 |
| | 0.0679 | 8.34 | 0.490 |
| | 0.0955 | 4.79 | 0.523 |
| | 0.1395 | 2.39 | 0.539 |
| | 0.1945 | 1.33 | 0.561 |
| | 0.2660 | 0.845 | 0.611 |
| | 0.3840 | 0.519 | 0.692 |
| | 0.6450 | 0.273 | 0.843 |
| 0.200 | 0.0235 | 21.82 | 0.549 |
| | 0.0347 | 11.65 | 0.592 |
| | 0.0469 | 6.07 | 0.578 |
| | 0.0676 | 3.38 | 0.621 |
| | 0.0954 | 2.05 | 0.683 |
| | 0.1399 | 1.10 | 0.734 |
| | 0.1940 | 0.743 | 0.836 |
| | 0.2160 | 0.472 | 0.742 |
| | 0.3820 | 0.279 | 1.009 |
| | 0.5380 | 0.172 | 1.116 |
| | 0.7450 | 0.127 | 1.33 |
| | 1.054 | 0.0982 | 1.65 |
| | 1.580 | 0.0758 | 2.18 |

bulk of the solution (2). The calculation of the amount of substance adsorbed, $\Gamma$, from chronopotentiometric data essentially involves extrapolation of $i - \tau$ data to zero $\tau$ (or infinite $i$) where the relative contribution of the solution species to the transition time becomes zero. The actual $\Gamma$ calculated however, depends upon the particular model used for this extrapolation. Different assumptions concerning the relative order of electrolysis of diffusing and adsorbed species, as well as different adsorption isotherms assumed in the treatment, lead to somewhat different values of $\Gamma$. Several models proposed for these calculations are discussed below.

## THEORETICAL MODELS

Several theoretical models for chronopotentiometry involving adsorption of the electroactive species were proposed by Lorenz (14); modifications of these were given by several other authors. The numbering system below generally corresponds to that given by Lorenz.

**1. Adsorbed Layer Electrolyzed First.** If the total current goes exclusively to electrolysis of the adsorbed layer, and after the adsorbed layer is depleted, exclusively to the diffusing substance until the transition time, $\tau$, is reached, the following equation is obtained (14)

$$i_o\tau = \frac{n^2F^2\pi D}{4}\frac{C^2}{i_o} + nF\Gamma \qquad (1)$$

A plot of $i_o\tau$ vs. $C^2/i_o$ results in a straight line of intercept $nF\Gamma$. This model was also suggested by Laitinen (12). Generally extrapolation by this procedure, for a given set of $i_o - \tau$ data, leads to the largest values of $\Gamma$.

**2. Adsorbed Layer Electrolyzed Last.** The total current here is assumed to go exclusively to the electrolysis of the diffusing species first. After the usual transition time for the diffusing species, $\tau_1$, the adsorbed species is electrolyzed. During the electrolysis of the adsorbed layer, the dissolved species continues to diffuse to the electrode, and the second transition time, $\tau_2$, is attained when the adsorbed layer is completely electrolyzed. An inflection will not necessarily be observed between these two transitions. Therefore, for a given amount of adsorbed species the total transition time is prolonged to a much greater extent than if the adsorbed species is electrolyzed first (model 1) or simultaneously with the diffusing species (models 3 and 4). For a given set of $i_o - \tau$ data, this model will lead to the smallest values of $\Gamma$.

Lorenz (14) performed an approximate treatment for this model, using the assumption that the current contributing to the electrolysis of the dif-
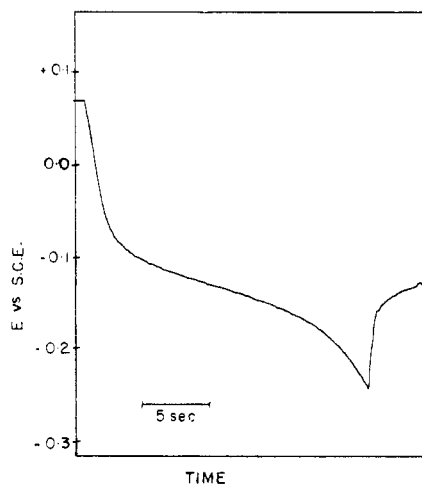


Figure 1. Chronopotentiogram for reduction of 0.40mM riboflavin in 0.5M NaHSO₄ and 1M Na₂SO₄ at current density of 0.0435 ma. per sq. cm.

fusing species during the electrolysis of the adsorbed layer varies as $t^{-1/2}$. With this assumption, the following equation was obtained:

$$(i_o\tau)^{1/2} = \frac{nF(\pi D)^{1/2}}{2}\frac{C}{i_o^{1/2}} + (nF\Gamma)^{1/2} \qquad (2)$$

A plot of $(i_o\tau)^{1/2}$ vs. $C/i_o^{1/2}$ yields a straight line of intercept $(nF\Gamma)^{1/2}$.

Since the equation relating the flux of the diffusing species after the first transition has been derived, the above approximation is unnecessary. A more rigorous derivation was given by Reinmuth (18) and Anson (1) in different, but equivalent, forms. The final equation is (18)

$$\frac{nF\pi\Gamma}{i_o} = \tau \arccos\left(\frac{\tau_1 - \tau_2}{\tau}\right) - 2(\tau_1\tau_2)^{1/2} \qquad (3)$$

where $\tau_1$ is the first transition time, due only to the diffusing species, and is given by

$$\tau_1 = n^2F^2\pi DC^2/4i_o^2 \qquad (4)$$

$$\tau = \tau_1 + \tau_2 \qquad (5)$$

Equations 3, 4, and 5 may be combined into a form somewhat more convenient for computation, and yield

$$y = \frac{x}{a}\arccos(2b/x - 1) - \frac{2}{a}[b(x - b)]^{1/2} \qquad (6)$$

where $y = i_o$, $x = i_o^2\tau$, $a = nF\pi\Gamma$, and $b = n^2F^2\pi C^2D/4$.

A plot of $x$ vs. $y$, extrapolated to $y = 0$, yields $x = b$, allowing the determination of $D$. Using this value for $D$, the value of $\Gamma$ for each $x$ and $y$ can be obtained.

**3. Simultaneous Electrolysis of Diffusing and Adsorbed Species—Constant Current.** A simple model for the simultaneous electrolysis of the adsorbed layer and the diffusing

species assumes that the fraction of the applied current contributing to both processes remains constant during the electrolysis. The following equation is obtained (14):

$$\frac{i_o\tau}{C} = \frac{nF(\pi D)^{1/2}}{2}\tau^{1/2} + \frac{nF\Gamma}{C} \qquad (7)$$

$\Gamma$ is calculated from the intercept of the line obtained by plotting $i_o\tau/C$ vs. $\tau^{1/2}$. Equation 7 has also been used to correct chronopotentiometric data for effects of oxide film reduction and double layer charging as well as adsorption (2).

**4. Simultaneous Electrolysis of Diffusing and Adsorbed Species—Linear Isotherm.** Lorenz derived an equation for simultaneous electrolysis assuming that the amount of adsorbed species present during electrolysis was linearly related to the concentration of the diffusing species at the electrode surface (14). Integration of the final equation given by Lorenz yields

$$\Gamma = \frac{2C(D\tau/\pi)^{1/2} - nFC^2D/i_o}{1 - \exp(a^2)\,\text{erfc}\,(a)} \qquad (8)$$

where $a = C(D\tau)^{1/2}/\Gamma$. Since Equation 8 is an implicit relation for $\Gamma$, its solution is only possible by an iterative method, after assuming a value of $D$. When $C(D\tau)^{1/2} >> \Gamma$, the term $\exp(a^2)\,\text{erfc}(a)$ approaches zero, and the equation may be written as:

$$C\tau^{1/2} = \frac{nF(\pi D)^{1/2}}{2}\frac{C^2}{i_o} + \frac{(\pi/D)^{1/2}\Gamma}{2} \qquad (9)$$

and $\Gamma$ can be calculated from the intercept of a plot of $C\tau^{1/2}$ vs. $C^2/i_o$. Equation 9 was used by Munson (16) for the determination of CO adsorbed on platinum.

**5. Other Models.** Various other models can be constructed based on other isotherms—e.g., the Langmuir isotherm. These generally lead to difficulties in solution of Fick's equation. All models based on isotherms assume that the rate of adsorption and desorption is sufficiently rapid that adsorption equilibrium is maintained during the electrolysis, while models 1, 2, 3 only require that adsorption equilibrium be established before the electrolysis. One method of determining the amount of adsorbed material independent of the theoretical model used for extrapolation involves experimentally increasing the current density, $i_o$, until the diffusion contribution becomes negligible and $i_o\tau$ becomes essentially constant. To calculate how short $\tau$ must be to bring about this condition, we can use the constant current model, model 3. As will be demonstrated below, calculations based on this model will be correct to within a factor of 2 or 3. For the contribution of the diffusing species to be

less than 10% of the adsorption contribution, we require that (Equation 7)

$$0.5nFC \ (D\pi\tau)^{1/2} < 0.1 \ nF\Gamma \qquad (10)$$

or, collecting constants and assuming a diffusion coefficient, $D$, of $1.0 \times 10^{-5}$ sq. cm. per second

$$\tau^{1/2} < 35.8\Gamma/C \text{ seconds} \qquad (11)$$

where $\Gamma$ is in moles per sq. cm. and $C$ is in moles per cubic centimeter. Assuming a $\Gamma$ of $1 \times 10^{-9}$ moles per sq. cm. (about or slightly more than one monolayer of adsorbed material) for bulk concentrations, $C$'s of 1 and 10m$M$, $\tau$'s of less than 1.3 msecond and 13 $\mu$second, respectively, must be used. Such short transition times are inconvenient, and in practice an extrapolation from somewhat longer times will often be practiced.

## DISCUSSION

**Chronopotentiometric Measurements.** Using the data for the chronopotentiometric reduction of riboflavin and the various theoretical models discussed, values of $\Gamma$ and $D$ were computed, and the results are shown in Table III. Data were plotted according to the procedures given in each model, and the calculations performed on a Control Data Corp. 1604 computer. Equations 1, 2, 7, and 9 were treated by a linear least squares analysis, obtaining $D$ from the line slopes and $\Gamma$ from the intercepts. The scatter of the data about the theoretical equations to which they are being fitted leads to somewhat different values of $D$ and $\Gamma$ if the data are treated differently. For example, if $i_o^2\tau/C^2$ is plotted against $i_o/C^2$ in model 1, so that $D$ is now obtained from the intercept and $\Gamma$ from the slope, values of $D$ of 0.5, 0.6, and $0.4 \times 10^{-5}$ sq. cm. per second, and values of $\Gamma$ of 1.1, 0.6, and 0.6 $\times 10^{-9}$ mole per sq. cm., for concentrations of riboflavin of 0.8, 0.4, and 0.2m$M$, respectively, are obtained. Similar, although somewhat smaller, differences are obtained from variations of data treatment in Equations 2, 7, and 9.

Equation 3 was treated using the extrapolation procedure described to obtain $D$, and then averaging the values
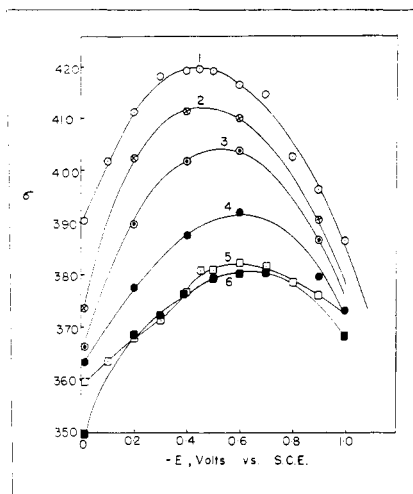


**Figure 2. Electrocapillary curves for 0.5M NaHSO₄–1M Na₂SO₄ buffer, pH 2**

1. 0mM riboflavin
2. 0.058mM
3. 0.11mM
4. 0.22mM
5. 0.45mM
6. 0.89mM

of $\Gamma$ obtained at each concentration. The approximation of Lorenz in model 2 leads to smaller values of $D$ and slightly larger values of $\Gamma$. Alternately, the values of $D$ found with the approximate model (Equation 2) in the more rigorous one (Equation 3) yields values of $\Gamma$ of 0.6, 0.5, and $0.4 \times 10^{-9}$ mole per sq. cm., for concentrations of 0.8, 0.4, and 0.2m$M$, respectively. Equation 8 was solved, using values of $D$ calculated by the approximate model (Equation 9), in a program employing an iterative procedure similar to one previously described (9). As expected, the values of $\Gamma$ calculated by model 1 are largest, those calculated by model 2 are smallest, and those obtained by models 3 and 4 are intermediate in magnitude.

**Electrocapillarity Measurements.** Electrocapillary curves for solutions of a bisulfate buffer, about pH 2, containing varying amounts of riboflavin are shown in Figure 2. The surface tension was determined by the drop time method, using the equation and the conditions suggested by Corbusier

and Gierst (7). The D.M.E. capillary was standardized in 0.1$M$ KNO₃, in which the interfacial tension between water and mercury is 378.3 dynes per cm. at $-0.011$ volt $vs$. S.C.E. (8). The determination of $\Gamma$ from electrocapillary curves, based on Gibb's adsorption equation is classical (17) and is based on the equation

$$\frac{d\sigma}{d\mu} = -\Gamma = \frac{d\sigma}{RT \ d\ln C} \qquad (12)$$

where $\sigma$ is the electrode-solution interfacial tension, and $\mu$ is the chemical potential in solution of the adsorbed substance. Equation 12 is based only on thermodynamic assumptions; the activity coefficient of riboflavin is assumed to be one. A plot of $\sigma$ against ln $C$ for concentrations of riboflavin between 0.058 and 0.89m$M$ at a potential of $-0.011$ volt $vs$. S.C.E. (corresponding to the foot of the chronopotentiometric wave) was essentially linear, and from a least squares calculation gave a $\Gamma$ of 0.33 ($\pm$0.04) $\times 10^{-9}$ mole per sq. cm.

By considering the size and shape of the riboflavin molecule and assuming various orientations of the molecule on the electrode surface, assuming rotation of the molecule and different orientations of the side chain, a monolayer consisting of about $0.2 \times 10^{-9}$ mole per sq. cm. was calculated.

## CONCLUSIONS

The value of $\Gamma$ obtained from chronopotentiometric measurements is dependent upon the model chosen for extrapolation. However $\Gamma$-values calculated by models 1 and 2 represent the two extremes in possible values, and those obtained by model 3 should be within a factor of two or three of values calculated by the other models. The best fit of the data to a single theoretical equation is probably not a good criterion for establishing which model is most correct. For all of the cases treated here, assuming $\Gamma$ and $D$ as two adjustable parameters in fitting the experimental data to the theoretical equations, the standard deviations were about the same. In general the value of $\Gamma$ obtained by chronopotentiometry agreed with that obtained by electrocapillarity measurements.

The polarographic reduction wave of riboflavin shows a pre-wave (4, 11), indicative of adsorption of the product of the electrode reaction. According to Brdička (4), adsorbed molecules are in a lower free energy state than those in solution, and hence are more difficult to reduce than molecules in solution. Under conditions where the product is not adsorbed, polarographic post-waves are obtained. Therefore, for reversible electrode reactions, one expects the diffusing species to be electrolyzed first,

**Table III. Amount of Riboflavin Adsorbed ($\Gamma$) and Diffusion Coefficient ($D$) Calculated by Different Theoretical Models**

| | $\Gamma \times 10^9$ mole per sq. cm. | | | | | | $D \times 10^5$ sq. cm. per second | | | | | |
|---|---|---|---|---|---|---|---|---|---|---|---|---|
| | Ads. layer electrolyzed first | | Adsorbed layer electrolyzed last | | | | Simultaneous electrolysis of adsorbed and diffusing species | | | | | |
| | Model 1 | | Model 2 | | Model 2a | | Model 3 | | Model 4 | | Model 4a | |
| $C$, m$M$ | $\Gamma$ | $D$ | $\Gamma$ | $D$ | $\Gamma$ | $D$ | $\Gamma$ | $D$ | $\Gamma$ | $D$ | $\Gamma$ | $D$ |
| 0.8 | 0.7 | 0.6 | 0.3 | 0.4 | 0.2 | 0.6 | 0.4 | 0.6 | 0.5 | 0.6 | 0.4 | 0.6 |
| 0.4 | 0.5 | 0.7 | 0.2 | 0.4 | 0.2 | 0.7 | 0.3 | 0.7 | 0.3 | 0.7 | 0.3 | 0.7 |
| 0.2 | 0.4 | 0.9 | 0.3 | 0.4 | 0.2 | 0.9 | 0.3 | 0.8 | 0.2 | 1.0 | 0.2 | 1.0 |

and then the adsorbed species. This will not necessarily hold for irreversible electrode reactions, where the adsorbed molecule may react more rapidly than the solution species. When only the product of an electrode reaction is adsorbed, polarographic pre-waves are obtained, since the reversible reduction of a substance to the adsorbed state requires less energy than reduction to the species in solution (4).

From polarographic studies, Brdička first assumed that only the product of the electroreduction of riboflavin—i.e., leuco-riboflavin—was adsorbed. More recent a.c. polarographic studies (5) present evidence for the adsorption of both riboflavin and leuco-riboflavin. Our studies support this idea; recent studies using current reversal chronopotentiometry (10) also indicate adsorption of leuco-riboflavin. The appearance of a pre-wave in this system provides evidence that the leuco-riboflavin is adsorbed more strongly than the riboflavin itself. Under these conditions the electrode reaction may proceed by the reduction of the diffusing riboflavin to form an adsorbed layer of the leucoform. As this adsorbed layer of leuco-riboflavin is formed, the adsorbed riboflavin is

desorbed and then reduced. If this mechanism is correct, the behavior of the system during chronopotentiometry is intermediate between models 2 and 3. No pre-wave was obtained on the chronopotentiometric reduction waves. We have no explanation for this effect. The electrochemical reduction of riboflavin is complicated by the formation of an intermediate free radical (semiquinone), and is being investigated further.

The chronopotentiometric measurement of adsorption has the advantage of being independent of the reversibility or irreversibility of the electrode reaction. Since several other possible effects can cause increases of $i_o \tau^{1/2}$ with decreasing $\tau$, particularly when solid electrodes are employed (2), interpretation of such increases as due solely to adsorption should be made with caution, and preferably independent methods of measuring adsorption should also be used.

### LITERATURE CITED

(1) Anson, F. C., ANAL. CHEM. **33**, 1123 (1961).
(2) Bard, A. J., *Ibid.*, **35**, 340 (1963).
(3) *Ibid.*, **33**, 11 (1961).
(4) Brdička, R., *Collection Czech. Chem. Commun.* **12**, 522 (1947).
(5) Breyer, B., Biegler, T., *Ibid.*, **25**, 3348 (1960).
(6) Brezina, M., Zuman, P., "Polarography in Medicine, Biochemistry, and Pharmacy," pp. 389–94, Interscience, New York, 1958.
(7) Corbusier, P., Gierst, L., *Anal. Chim. Acta* **15**, 254 (1956).
(8) Craxford, S. R., McKay, H. A. C., *J. Phys. Chem.* **39**, 545 (1935).
(9) Herman, H., Bard, A. J., ANAL. CHEM. **35**, 1121 (1963).
(10) Herman, H., Tatwawadi, S. V., Bard, A. J., *Ibid.*, **35**, 2210 (1963).
(11) Kolthoff, I. M., Lingane, J. J., "Polarography," pp. 256, 844, Interscience, New York, 1952.
(12) Laitinen, H. A., ANAL. CHEM. **33**, 1458 (1961).
(13) Landsberg, R., Nitzche, R., Geissler, W., *Z. Physik. Chem. Leipzig* **222**, 54 (1963).
(14) Lorenz, W., *Z. Elektrochem.* **59**, 730 (1955).
(15) Lorenz, W., Mühlberg, H., *Ibid.* **59**, 736 (1955); *Z. physik. Chem. Frankfurt* **17**, 129 (1958).
(16) Munson, R. A., *J. Electroanal. Chem.* **5**, 292 (1963).
(17) Parsons, R., "Modern Aspects of Electrochemistry," J. O'M. Bockris, ed., pp. 128–34, Butterworths, London, 1954.
(18) Reinmuth, W. H., ANAL. CHEM. **33**, 322 (1961).

# A Chronopotentiometric Study of Adsorption

**H. A. LAITINEN and L. M. CHAMBERS[1]**

*Noyes Chemical Laboratory, University of Illinois, Urbana, Ill.*

▶ The chronopotentiometric method is a sensitive qualitative indication of adsorption. Quantitative determination of surface excess of Alizarin Red S failed because of the current required for the desorption of reduction product. Using tris(ethylenediamine) cobalt(III) and (II) ions, three equations, representing different physical models for the electrode reaction of the solution phase and the surface excess, were tested. All indicated a small amount of adsorption, but no choice could be made among the models. Several limitations on the quantitative study of adsorption by chronopotentiometry are pointed out.

CHRONOPOTENTIOMETRY has been used by only a few workers for the investigation of adsorption of reactants (1–4, 10, 16, 17, 21). When short transition times are used, it is particularly important to establish the presence or absence of an adsorbed phase, because even a fractional monolayer of adsorbed reactant can rep-

resent an appreciable portion of the entire electrolysis process (10).

Of the many possible theoretical models that might be set up to describe the simultaneous or sequential reduction or oxidation of adsorbed and diffusing phases, three are particularly amenable to experimental investigation. The first model (10, 16, 21) assumes the additivity of transition times,

$$\tau = \tau_a + \tau_d \qquad (1)$$

as would be observed if the adsorbed phase were electrolyzed first in a time $\tau_a$, followed by the electrolysis of the diffusing species to bring its surface concentration to zero in time $\tau_d$. If $I$ is the applied current density, then

$$I\tau_a = nF\Gamma \qquad (2)$$

where $\Gamma$ is the surface concentration of adsorbate in moles per square centimeter.

By adding $\tau_a$ to $\tau_d$, as given by the Sand equation for linear diffusion (24), we obtain

$$I\tau = nF\Gamma + \frac{(nFC)^2 \pi D}{4I} \qquad (3)$$

A plot of $I\tau$ vs. $1/I$ should be linear, according to this model, with an intercept $nF\Gamma$ which can be used to determine surface excess (10) and a slope proportional to $C^2 D$.

The second model (4, 16, 21) assumes a simultaneous reaction of adsorbed and diffusing phases in such a way that a constant fraction of the applied current goes to each phase during the entire electrolysis. Thus

$$I = I_a + I_d \qquad (4)$$

and

$$I\tau = nF\Gamma + \frac{nFC(\pi D\tau)^{1/2}}{2} \qquad (5)$$

According to this model, a plot of $I\tau$ vs. $\tau^{1/2}$ should be linear, with an intercept of $nF\Gamma$ and a slope proportional to $CD^{1/2}$.

The third model (15, 16) requires that the adsorbed layer be electrolyzed at the

---

[1] Present address, Ivorydale Technical Center, The Procter and Gamble Co., Cincinnati 17, Ohio.